

Quantum noise properties of an injection-locked laser oscillator with pump-noise suppression and squeezed injection

Lars Gillner and Gunnar Björk

Department of Microwave Engineering and Fibre Optics, Royal Institute of Technology, Box 70033, S-100 44 Stockholm, Sweden

Yoshihisa Yamamoto

NTT Basic Research Laboratories, 3-9-11 Midori-cho, Musashino-shi, 180 Tokyo, Japan

(Received 5 December 1989)

The quantum noise properties of injection-locked semiconductor laser oscillators are investigated. Included in the analysis are pump-noise suppression and squeezing of the injection signal. It is shown that the main effect of injection locking is the reduction of the phase noise of the outgoing laser light field. The influence that squeezing of the injection signal state has on the output state is shown to be strongly dependent on the value of the linewidth enhancement factor. In general, little or no noise reduction stands to be gained by squeezing the injection signal. It is also shown that under idealized conditions, the spectral uncertainty product of the outgoing field will approach, but never go below, the minimum uncertainty value given by the Heisenberg uncertainty relation.

I. INTRODUCTION

In recent years the redistribution and suppression of optical quantum noise have been drawing considerable attention.¹⁻³ Several authors⁴⁻⁷ have calculated the noise properties of lasers that are pumped by noncoherent fields or that have the vacuum fields incident on the open port replaced by squeezed vacuum. In this paper we have calculated the amplitude and phase noise spectra of an injection-locked semiconductor laser oscillator. Here, an injection-locked laser is a laser that is forced to oscillate at the frequency of an optical injection signal. The laser may be pumped by a noise suppressed current and the injection signal may be in a squeezed state. (The input field may even be a squeezed vacuum state, although such an operating mode can hardly qualify as injection locking.) From the external field spectra, the spectral uncertainty product has been calculated. An earlier treatment of the quantum noise properties of an injection-locked laser can be found in Ref. 8.

Specifically two important questions are addressed in this paper. It is known that reducing the pump noise in a laser will result in amplitude fluctuations in the signal lower than the standard quantum limit.⁴ It is also known that injection locking of a laser can reduce the phase noise of the signal by several orders of magnitude.⁸ Combining these techniques, is it possible to reduce the phase noise of the laser while maintaining the amplitude noise level of a free-running pump-noise suppressed laser? The answer is no, and thus, Heisenberg's uncertainty relation cannot be violated. The next important question is if the phase noise of an injection-locked laser can be further reduced by squeezing the phase noise of the injection signal. The answer is yes, but the phase-noise reduction is only a small amount. Heisenberg's uncertainty relation is preserved in this case as well.

We have concentrated our efforts on semiconductor

laser oscillators, the most notable difference from gas lasers being the coupling between the real and imaginary parts of the electric susceptibility operator in the former case.⁹ This coupling seriously degrades the phase noise performance of a nonideal semiconductor laser as compared to an ideal one, lacking this coupling. It is known that the inclusion of this coupling is of utmost importance in applying theory to predict experimental results. In our calculations no attention has been paid to the dynamical stability of the solutions obtained. As shown in a number of papers,¹⁰⁻¹³ the locking bandwidth predicted by a linearized analysis is greater than the bandwidth over which stable injection locking actually is possible.

The calculations performed in this paper are based on the model presented in Ref. 14. This model, graphically shown in Fig. 1, assumes that the laser's rear mirror reflectivity is equal to unity. Thus the cavity couples to one external field mode only. In addition, the reflectivity of the front mirror is assumed to be close to unity.

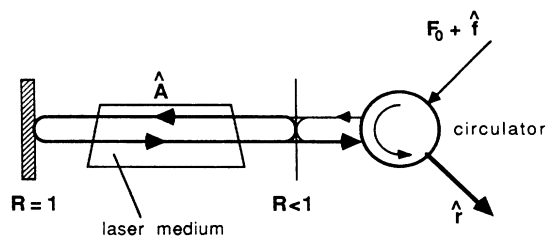


FIG. 1. Model of an injection-locked laser oscillator. \hat{A} is the internal field, $F_0 + \hat{f}$ is the injection signal, and \hat{r} is the output field.

II. LANGEVIN EQUATIONS

In order to analyze an injection-locked laser oscillator, first we establish the Langevin equations for the internal photon field, the dipole moment, and the electron system for a laser with an injection signal. Then we use the relation between the internal and external photon fields together with the correlation functions between the different noise sources to calculate the internal and external amplitude and phase-noise spectral densities.

A. Internal field

The Langevin equation for the internal field $\hat{A}(t)$ is given by¹⁴

$$\begin{aligned} \frac{d\hat{A}(t)}{dt} = & -\frac{1}{2} \left[\frac{\omega}{Q} + i2\omega_r - \frac{\omega}{\mu^2} (\tilde{\chi}_i - i\tilde{\chi}_r) \right] \hat{A}(t) \\ & + \left[\left[\frac{\omega}{\mu^2} \langle \tilde{\chi}_i \rangle \right]^{1/2} \tilde{f}_G(t) + \left[\frac{\omega}{Q_0} \right]^{1/2} \tilde{f}_L(t) \right. \\ & \left. + \left[\frac{\omega}{Q_e} \right]^{1/2} [F_0 + \hat{f}(t)] \right] e^{-i\omega t}, \quad (2.1) \end{aligned}$$

where we have introduced $F_0 + \hat{f}(t)$ as the amplitude of the injection signal. Here F_0 is the classical excitation and $\hat{f}(t)$ is a fluctuation operator. Depending on the choice of F_0 and $\hat{f}(t)$, the injection signal may be a vacuum state, a coherent state, or a squeezed state. The optical angular frequency of the injection signal is denoted by ω . The total Q value Q of the laser cavity depends on the external (mirror) losses Q_e and the internal losses Q_0 according to

$$\frac{1}{Q} = \frac{1}{Q_e} + \frac{1}{Q_0}. \quad (2.2)$$

The angular resonance frequency of the unpumped cavity is denoted ω_r , μ is the refractive index, and $\tilde{\chi}$ is the electronic susceptibility operator, whose imaginary part equals the stimulated emission gain:

$$\frac{\omega}{\mu^2} \tilde{\chi}_i = \tilde{E}_{cv} - \tilde{E}_{vc}, \quad (2.3)$$

where \tilde{E}_{cv} and \tilde{E}_{vc} are the operators of the stimulated emission and absorption rates, respectively. The noise operators $\tilde{f}_G(t)$, $\tilde{f}_L(t)$, and $\hat{f}(t)$ are associated with the gain mechanism, the internal losses, and the injection signal fluctuations, respectively. We use a tilde to denote operators for the electron system and a circumflex to denote operators for the photon field system.

The Langevin equation for the total excited electron number operator $\tilde{N}_c(t)$ is given by¹⁴

$$\begin{aligned} \frac{d\tilde{N}_c(t)}{dt} = & p - \frac{\tilde{N}_c(t)}{\tau_{sp}} - (\tilde{E}_{cv} - \tilde{E}_{vc}) \hat{n}(t) - \langle \tilde{E}_{cv} \rangle \\ & + \tilde{\Gamma}_p(t) + \tilde{\Gamma}_{sp}(t) + \tilde{\Gamma}(t), \quad (2.4) \end{aligned}$$

where p is the pumping rate, τ_{sp} is the lifetime of the electrons due to spontaneous emission, and $\hat{n}(t) \equiv \hat{A}^\dagger(t) \hat{A}(t)$ is the photon number operator. The three last terms in

Eq. (2.4) are fluctuating noise operators: $\tilde{\Gamma}_p(t)$ is the pump noise, $\tilde{\Gamma}_{sp}(t)$ is the spontaneous emission noise, and $\tilde{\Gamma}(t)$ is the dipole moment fluctuation noise.

For the noise sources in Eqs. (2.1) and (2.4) we use the shorter notations

$$\begin{aligned} \hat{H}(t) = & \left[\frac{\omega}{\mu^2} \langle \tilde{\chi}_i \rangle \right]^{1/2} \tilde{f}_G(t) + \left[\frac{\omega}{Q_0} \right]^{1/2} \tilde{f}_L(t) \\ & + \left[\frac{\omega}{Q_e} \right]^{1/2} \hat{f}(t), \quad (2.5) \end{aligned}$$

$$\tilde{F}_c(t) = \tilde{\Gamma}_p(t) + \tilde{\Gamma}_{sp}(t) + \tilde{\Gamma}(t). \quad (2.6)$$

In order to analyze Eqs. (2.1) and (2.4) we expand the operators into mean and fluctuating parts according to

$$\tilde{N}_c(t) = N_{c0} + \Delta\tilde{N}_c(t), \quad (2.7)$$

$$\hat{A}(t) = [A_0 + \Delta\hat{A}(t)] e^{-i[\omega t + \phi_0 + \Delta\hat{\phi}(t)]}, \quad (2.8)$$

$$\begin{aligned} \hat{n}(t) = \hat{A}^\dagger(t) \hat{A}(t) \approx & [A_0 + \Delta\hat{A}(t)]^2 \\ \approx & A_0^2 + 2A_0\Delta\hat{A}(t), \quad (2.9) \end{aligned}$$

$$\tilde{\chi}_i = \langle \tilde{\chi}_i \rangle + \frac{d\langle \tilde{\chi}_i \rangle}{dN_{c0}} \Delta\tilde{N}_c, \quad (2.10)$$

$$\tilde{\chi}_r = \langle \tilde{\chi}_r \rangle + \frac{d\langle \tilde{\chi}_r \rangle}{dN_{c0}} \Delta\tilde{N}_c. \quad (2.11)$$

Here N_{c0} , A_0 , and ϕ_0 are the average excited electron number, field amplitude, and phase (c numbers). $\Delta\tilde{N}_c$, $\Delta\hat{A}$, and $\Delta\hat{\phi}$ are the Hermitian excited electron number, field amplitude, and phase operators. Although this Hermitian phase operator is not correct in a strict quantum-mechanical sense, cf. Ref. 15, it is known that Eq. (2.8) is a good approximation when the photon number A_0^2 is much larger than unity.

We also introduce the notations

$$\frac{1}{\tau_{st}} = \frac{\omega}{\mu^2} A_0^2 \frac{d\langle \tilde{\chi}_i \rangle}{dN_{c0}}, \quad (2.12)$$

$$\omega_0 = \omega_r + \frac{\omega}{2\mu^2} \langle \tilde{\chi}_r \rangle, \quad (2.13)$$

$$\alpha = \frac{d\langle \tilde{\chi}_r \rangle}{dN_{c0}} / \frac{d\langle \tilde{\chi}_i \rangle}{dN_{c0}}, \quad (2.14)$$

$$\beta = \frac{\langle \tilde{E}_{cv} \rangle}{N_{c0}/\tau_{sp}}, \quad (2.15)$$

$$n_{sp} = \frac{\langle \tilde{E}_{cv} \rangle}{\langle \tilde{E}_{cv} \rangle - \langle \tilde{E}_{vc} \rangle}, \quad (2.16)$$

and

$$G = \frac{\omega}{\mu^2} \langle \tilde{\chi}_i \rangle, \quad (2.17)$$

where τ_{st} is the electron lifetime due to stimulated emission, ω_0 is the resonance angular frequency of the pumped cavity including the frequency shift introduced by the injection, α is the linewidth enhancement factor, β

is the spontaneous emission factor, n_{sp} is the population inversion factor, and G is the average of the stimulated emission gain. The Q values are replaced by photon lifetimes according to

$$\frac{1}{\tau_{p0}} = \frac{\omega}{Q_0}, \quad \frac{1}{\tau_{pe}} = \frac{\omega}{Q_e}, \quad \frac{1}{\tau_p} = \frac{\omega}{Q}. \quad (2.18)$$

Two steady-state equations are obtained from the nonfluctuating real and imaginary parts of Eq. (2.1) using Eqs. (2.5), (2.8), (2.10)–(2.14), (2.17), and (2.18):

$$G = \frac{1}{\tau_p} - 2 \frac{F_0}{A_0} \left[\frac{1}{\tau_{pe}} \right]^{1/2} \cos \phi_0, \quad (2.19)$$

$$\omega - \omega_0 = - \frac{F_0}{A_0} \left[\frac{1}{\tau_{pe}} \right]^{1/2} \sin \phi_0. \quad (2.20)$$

Equation (2.13) can be rewritten, with the help of Eqs. (2.14), (2.17), and (2.19), as

$$\begin{aligned} \omega_0 &= \omega_r + \frac{\omega}{2\mu^2} \left[\langle \tilde{\chi}_r \rangle \Big|_{G=1/\tau_p} + \frac{d\langle \tilde{\chi}_r \rangle}{dG} \left(G - \frac{1}{\tau_p} \right) \right] \\ &= \omega_{r0} + \frac{\alpha}{2} \left[G - \frac{1}{\tau_p} \right] \\ &= \omega_{r0} - \alpha \frac{F_0}{A_0} \left[\frac{1}{\tau_{pe}} \right]^{1/2} \cos \phi_0, \end{aligned} \quad (2.21)$$

Thus ω_{r0} is the resonance angular frequency for the pumped cavity, when the laser is lasing in the absence of any injection signal, since $F_0=0$ implies that $G=1/\tau_p$. In the following calculations ω_{r0} is constant. The detuning parameter $\Delta\omega$ is defined as the angular frequency difference between the injection signal angular frequency ω and the resonance angular frequency of the cavity ω_{r0} . Together with Eqs. (2.20) and (2.21) it is expressed as

$$\Delta\omega \equiv \omega - \omega_{r0} = -(\sin \phi_0 + \alpha \cos \phi_0) \frac{F_0}{A_0} \left[\frac{1}{\tau_{pe}} \right]^{1/2}. \quad (2.22)$$

Equation (2.22) gives the possible locking bandwidth

$$-(1 + \alpha^2)^{1/2} \frac{F_0}{A_0} \left[\frac{1}{\tau_{pe}} \right]^{1/2} \leq \Delta\omega \leq \frac{F_0}{A_0} \left[\frac{1}{\tau_{pe}} \right]^{1/2}. \quad (2.23)$$

This bandwidth is obtained by noting that the condition $G - 1/\tau_p \leq 0$ must be fulfilled,¹³ implying that $-\pi/2 \leq \phi_0 \leq \pi/2$. When $\alpha \neq 0$, the detuning range becomes asymmetric, cf., for instance, Refs. 10, 11, and 13.

The nonfluctuating part of Eq. (2.4), together with Eqs. (2.3), (2.6), (2.7), (2.9), (2.10), (2.12), (2.15), and (2.17), results in the steady-state equation

$$p = (1 + \beta) \frac{N_{c0}}{\tau_{sp}} + G A_0^2. \quad (2.24)$$

A normalized pumping parameter R can then be defined by

$$R \equiv \frac{p}{p_{th0}} - 1 \quad (2.25)$$

where

$$p_{th0} \equiv (1 + \beta) \frac{N_{c0}}{\tau_{sp}}, \quad (2.26)$$

which is the threshold pumping rate for the free-running laser. An expression for τ_{st} can then be obtained by assuming a linear dependence of the gain on electron number:

$$\frac{1}{\tau_{st}} = \frac{R n_{sp}}{\tau_{sp}}. \quad (2.27)$$

The fluctuating part of Eq. (2.4) and the fluctuating real and imaginary parts of Eq. (2.1) give the following linearized equations for the noise operators, when the terms in the order of Δ^2 have been neglected:

$$\frac{d}{dt} \Delta \tilde{N}_c(t) = A_1 \Delta \tilde{N}_c(t) + A_2 \Delta \hat{A}(t) + \tilde{F}_c(t), \quad (2.28)$$

$$\frac{d}{dt} \Delta \hat{A}(t) = A_3 \Delta \tilde{N}_c(t) - A_5 \Delta \hat{A}(t) - A_0 A_6 \Delta \hat{\phi}(t) + \hat{H}_r(t), \quad (2.29)$$

$$\frac{d}{dt} \Delta \hat{\phi}(t) = A_4 \Delta \tilde{N}_c(t) + \frac{A_6}{A_0} \Delta \hat{A}(t) - A_5 \Delta \hat{\phi}(t) - \frac{1}{A_0} \hat{H}_i(t), \quad (2.30)$$

where

$$A_1 = -\frac{1}{\tau_{sp}} - \frac{1}{\tau_{st}}, \quad (2.31)$$

$$A_2 = -2 A_0 G, \quad (2.32)$$

$$A_3 = \frac{1}{2 A_0 \tau_{st}}, \quad (2.33)$$

$$A_4 = \frac{\alpha}{2 A_0^2 \tau_{st}}, \quad (2.34)$$

$$A_5 = \frac{F_0}{A_0} \left[\frac{1}{\tau_{pe}} \right]^{1/2} \cos \phi_0, \quad (2.35)$$

$$A_6 = \frac{F_0}{A_0} \left[\frac{1}{\tau_{pe}} \right]^{1/2} \sin \phi_0. \quad (2.36)$$

The operators \hat{H}_r and \hat{H}_i are the Hermitian quadrature noise operators:

$$\hat{H}_r = \frac{1}{2} (\hat{H} e^{i[\phi_0 + \Delta \hat{\phi}(t)]} + \hat{H}^\dagger e^{-i[\phi_0 + \Delta \hat{\phi}(t)]}), \quad (2.37)$$

$$\hat{H}_i = \frac{1}{2i} (\hat{H} e^{i[\phi_0 + \Delta\hat{\phi}(t)]} - \hat{H}^\dagger e^{-i[\phi_0 + \Delta\hat{\phi}(t)]}) . \quad (2.38)$$

Fourier transforming Eqs. (2.28)–(2.30) gives

$$i\Omega\Delta\tilde{N}_c(\Omega) = A_1\Delta\tilde{N}_c(\Omega) + A_2\Delta\hat{A}(\Omega) + \tilde{F}_c(\Omega) , \quad (2.39)$$

$$i\Omega\Delta\hat{A}(\Omega) = A_3\Delta\tilde{N}_c(\Omega) - A_5\Delta\hat{A}(\Omega) - A_0A_6\Delta\hat{\phi}(\Omega) + \hat{H}_r(\Omega) , \quad (2.40)$$

$$i\Omega\Delta\hat{\phi}(\Omega) = A_4\Delta\tilde{N}_c(\Omega) + \frac{A_6}{A_0}\Delta\hat{A}(\Omega) - A_5\Delta\hat{\phi}(\Omega)$$

$$- \frac{1}{A_0}\hat{H}_i(\Omega) . \quad (2.41)$$

From these equations $\tilde{N}_c(\Omega)$ is eliminated and expressions for the internal amplitude and phase noise $\Delta\hat{A}(\Omega)$ and $\Delta\hat{\phi}(\Omega)$ are obtained as

$$\Delta\hat{A}(\Omega) = \frac{(B_3 + iB_4)\tilde{F}_c(\Omega) + (B_5 + iB_6)\hat{H}_i(\Omega) + (B_7 + iB_8)\hat{H}_r(\Omega)}{B_1 + iB_2} , \quad (2.42)$$

$$\Delta\hat{\phi}(\Omega) = \frac{(B_{11} + iB_{12})\tilde{F}_c(\Omega) + (B_{15} + iB_{16})\hat{H}_i(\Omega) + (B_{13} + iB_{14})\hat{H}_r(\Omega)}{B_9 + iB_{10}} . \quad (2.43)$$

The expressions for the B coefficients are given in the Appendix.

B. External field

The output wave $\hat{r}(t)$ is related to the internal field $\hat{A}(t)$ and the injection signal F_0 through¹⁴

$$\hat{r}(t) = -[F_0 + \hat{f}(t)] + \left[\frac{\omega}{Q_e} \right]^{1/2} \hat{A}(t) . \quad (2.44)$$

As in the case of the internal field calculations, the operators are expanded according to

$$\hat{r}(t) = [r_0 + \Delta\hat{r}(t)] e^{-i[\psi_0 + \Delta\hat{\psi}(t)]} , \quad (2.45)$$

$$\hat{A}(t) = [A_0 + \Delta\hat{A}(t)] e^{-i[\phi_0 + \Delta\hat{\phi}(t)]} . \quad (2.46)$$

The phase ψ_0 of the external field has to be introduced, since in the case of nonzero injection, the internal and external fields do not have the same phase. The steady-state solution of (2.44)–(2.46) is

$$r_0 = \left[\frac{1}{\tau_{pe}} A_0^2 + F_0^2 - 2F_0 A_0 \left[\frac{1}{\tau_{pe}} \right]^{1/2} \cos\phi_0 \right]^{1/2} . \quad (2.47)$$

The equations for the fluctuating parts are (when ψ_0 has been expressed in ϕ_0)

$$\frac{C_4}{r_0} \Delta\hat{r}(t) + C_3 [\Delta\hat{\phi}(t) - \Delta\hat{\psi}(t)] = -\hat{f}_r(t) + C_1 \Delta\hat{A}(t) , \quad (2.48)$$

$$-\frac{C_3}{r_0} \Delta\hat{r}(t) + C_4 [\Delta\hat{\phi}(t) - \Delta\hat{\psi}(t)] = -\hat{f}_i(t) - C_2 \Delta\hat{A}(t) - F_0 \Delta\hat{\phi}(t) , \quad (2.49)$$

where we have introduced

$$C_1 = \left[\frac{1}{\tau_{pe}} \right]^{1/2} \cos\phi_0 , \quad (2.50)$$

$$C_2 = \left[\frac{1}{\tau_{pe}} \right]^{1/2} \sin\phi_0 , \quad (2.51)$$

$$C_3 = A_0 C_2 , \quad (2.52)$$

$$C_4 = A_0 C_1 - F_0 , \quad (2.53)$$

$$\hat{f}_r = \frac{1}{2} (\hat{f} e^{i\Delta\hat{\phi}(t)} + \hat{f}^\dagger e^{-i\Delta\hat{\phi}(t)}) , \quad (2.54)$$

$$\hat{f}_i = \frac{1}{2i} (\hat{f} e^{i\Delta\hat{\phi}(t)} - \hat{f}^\dagger e^{-i\Delta\hat{\phi}(t)}) . \quad (2.55)$$

In the absence of an injection signal $\phi_0 \equiv 0$ must be used to obtain the correct equations for a free-running laser, cf. Eqs. (5.1) and (5.2) in Ref. 14. The solutions for the external amplitude and phase noise $\Delta\hat{r}(\Omega)$ and $\Delta\hat{\psi}(\Omega)$ of Eqs. (2.48) and (2.49) are

$$\Delta\hat{r}(\Omega) = C_8 [C_9 \Delta\hat{A}(\Omega) + C_{10} \Delta\hat{\phi}(\Omega) + C_{11} \hat{f}_r(\Omega) + C_{12} \hat{f}_i(\Omega)] , \quad (2.56)$$

$$\Delta\hat{\psi}(\Omega) = C_5 [C_6 \Delta\hat{A}(\Omega) + C_7 \Delta\hat{\phi}(\Omega) + C_3 \hat{f}_r(\Omega) + C_4 \hat{f}_i(\Omega)] . \quad (2.57)$$

In these equations $\Delta\hat{A}(\Omega)$ and $\Delta\hat{\phi}(\Omega)$ can be substituted by the expressions in Eqs. (2.42) and (2.43). In order to obtain the noise spectra, the correlation functions between the noise operators have to be known. They can be deduced as¹⁴

$$\langle \hat{H}_r(t) \hat{H}_r(u) \rangle = \frac{1}{4} \left[\left[\frac{1}{\kappa\tau_{pe}} + \frac{1}{\tau_{p0}} \right] (1 + 2n_{th}) + \langle \tilde{E}_{cv} \rangle + \langle \tilde{E}_{vc} \rangle \right] \delta(t - u) , \quad (2.58)$$

$$\langle \hat{H}_i(t) \hat{H}_i(u) \rangle = \frac{1}{4} \left[\left[\frac{\kappa}{\tau_{pe}} + \frac{1}{\tau_{p0}} \right] (1 + 2n_{th}) + \langle \tilde{E}_{cv} \rangle + \langle \tilde{E}_{vc} \rangle \right] \delta(t - u) , \quad (2.59)$$

$$\langle \tilde{F}_c(t) \tilde{F}_c(u) \rangle = \left[p + \frac{N_{c0}}{\tau_{sp}} + \langle \tilde{E}_{cv} \rangle (A_0^2 + 1) + \langle \tilde{E}_{vc} \rangle A_0^2 \right] \delta(t - u) , \quad (2.60)$$

$$\langle \bar{F}_c(t) \hat{H}_r(u) \rangle = -\frac{A_0}{2} [\langle \bar{E}_{cv} \rangle + \langle \bar{E}_{vc} \rangle] \delta(t-u), \quad (2.61)$$

$$\langle \bar{F}_c(t) \hat{H}_i(u) \rangle = 0, \quad (2.62)$$

$$\langle \hat{H}_r(t) \hat{H}_i(u) \rangle + \langle \hat{H}_i(t) \hat{H}_r(u) \rangle \equiv 0, \quad (2.63)$$

$$\langle \hat{f}_r(t) \hat{f}_r(u) \rangle = \frac{1}{4\kappa} (1+2n_{th}) \delta(t-u), \quad (2.64)$$

$$\langle \hat{f}_i(t) \hat{f}_i(u) \rangle = \frac{\kappa}{4} (1+2n_{th}) \delta(t-u), \quad (2.65)$$

$$\langle \hat{f}_r(t) \hat{f}_i(u) \rangle + \langle \hat{f}_i(t) \hat{f}_r(u) \rangle \equiv 0, \quad (2.66)$$

$$\begin{aligned} \langle \hat{H}_r(t) \hat{f}_r(u) \rangle &= \langle \hat{f}_r(t) \hat{H}_r(u) \rangle \\ &= \frac{1}{4\kappa} \left[\frac{1}{\tau_{pe}} \right]^{1/2} (1+2n_{th}) (\cos\phi_0) \delta(t-u), \end{aligned} \quad (2.67)$$

$$\begin{aligned} \langle \hat{H}_i(t) \hat{f}_r(u) \rangle &= \langle \hat{f}_r(t) \hat{H}_i(u) \rangle \\ &= \frac{1}{4} \left[\frac{1}{\tau_{pe}} \right]^{1/2} (1+2n_{th}) (\sin\phi_0) \delta(t-u), \end{aligned} \quad (2.68)$$

$$\begin{aligned} \langle \hat{H}_r(t) \hat{f}_i(u) \rangle &= \langle \hat{f}_i(t) \hat{H}_r(u) \rangle \\ &= -\frac{1}{4} \left[\frac{1}{\tau_{pe}} \right]^{1/2} (1+2n_{th}) (\sin\phi_0) \delta(t-u), \end{aligned} \quad (2.69)$$

$$\begin{aligned} \langle \hat{H}_i(t) \hat{f}_i(u) \rangle &= \langle \hat{f}_i(t) \hat{H}_i(u) \rangle \\ &= \frac{\kappa}{4} \left[\frac{1}{\tau_{pe}} \right]^{1/2} (1+2n_{th}) (\cos\phi_0) \delta(t-u). \end{aligned} \quad (2.70)$$

The factor κ is the squeezing factor of the injection signal. If the injection signal is in a coherent state, κ equals unity. However, if the quantum noise of the injection signal has been redistributed by squeezing, κ can take on any positive value. Reduced amplitude (in-phase) noise in the input signal is characterized by $\kappa > 1$, and reduced phase (quadrature-phase) noise is characterized by $\kappa < 1$.

The quantity n_{th} is the number of thermally generated photons, which is approximately equal to zero at room temperature and optical frequencies:

$$n_{th} = (e^{\hbar\omega/kT} - 1)^{-1} \approx 0. \quad (2.71)$$

From (2.3) and (2.15)–(2.17) the stimulated emission and absorption rates are calculated as

$$\langle \bar{E}_{cv} \rangle = G n_{sp}, \quad (2.72)$$

$$\langle \bar{E}_{vc} \rangle = G (n_{sp} - 1). \quad (2.73)$$

Finally, the resulting expressions for the internal and external amplitude and phase-noise spectral densities are

given by

$$\begin{aligned} P_{\Delta\hat{A}}(\Omega) &= \langle \hat{A}^\dagger(\Omega) \hat{A}(\Omega) \rangle \\ &= \frac{(B_3^2 + B_4^2) P_{\bar{F}_c}(\Omega) + (B_5^2 + B_6^2) P_{\hat{H}_i}(\Omega) + (B_7^2 + B_8^2) P_{\hat{H}_r}(\Omega) + 2(B_3 B_7 + B_4 B_8) \langle \bar{F}_c(\Omega) \hat{H}_r(\Omega) \rangle}{B_1^2 + B_2^2}, \end{aligned} \quad (2.74)$$

$$\begin{aligned} P_{\Delta\hat{\phi}}(\Omega) &= \frac{(B_{11}^2 + B_{12}^2) P_{\bar{F}_c}(\Omega) + (B_{15}^2 + B_{16}^2) P_{\hat{H}_i}(\Omega) + (B_{13}^2 + B_{14}^2) P_{\hat{H}_r}(\Omega) + 2(B_{11} B_{13} + B_{12} B_{14}) \langle \bar{F}_c(\Omega) \hat{H}_r(\Omega) \rangle}{B_9^2 + B_{10}^2}, \end{aligned} \quad (2.75)$$

$$\begin{aligned} P_{\Delta\hat{r}}(\Omega) &= (D_7^2 + D_8^2) P_{\bar{F}_c}(\Omega) + (D_{11}^2 + D_{12}^2) P_{\hat{H}_i}(\Omega) + (D_9^2 + D_{10}^2) P_{\hat{H}_r}(\Omega) \\ &\quad + C_8^2 [C_{11}^2 P_{\hat{f}_r}(\Omega) + C_{12}^2 P_{\hat{f}_i}(\Omega)] + 2(D_7 D_9 + D_8 D_{10}) \langle \bar{F}_c(\Omega) \hat{H}_r(\Omega) \rangle \\ &\quad + 2C_8 [C_{11} D_9 \langle \hat{H}_r(\Omega) \hat{f}_r(\Omega) \rangle + C_{11} D_{11} \langle \hat{H}_i(\Omega) \hat{f}_r(\Omega) \rangle + C_{12} D_9 \langle \hat{H}_r(\Omega) \hat{f}_i(\Omega) \rangle + C_{12} D_{11} \langle \hat{H}_i(\Omega) \hat{f}_i(\Omega) \rangle], \end{aligned} \quad (2.76)$$

$$\begin{aligned} P_{\Delta\hat{\psi}}(\Omega) &= (D_1^2 + D_2^2) P_{\bar{F}_c}(\Omega) + (D_5^2 + D_6^2) P_{\hat{H}_i}(\Omega) + (D_3^2 + D_4^2) P_{\hat{H}_r}(\Omega) \\ &\quad + C_5^2 [C_3^2 P_{\hat{f}_r}(\Omega) + C_4^2 P_{\hat{f}_i}(\Omega)] + 2(D_1 D_3 + D_2 D_4) \langle \bar{F}_c(\Omega) \hat{H}_r(\Omega) \rangle \\ &\quad + 2C_5 [C_3 D_3 \langle \hat{H}_r(\Omega) \hat{f}_r(\Omega) \rangle + C_3 D_5 \langle \hat{H}_i(\Omega) \hat{f}_r(\Omega) \rangle + C_4 D_3 \langle \hat{H}_r(\Omega) \hat{f}_i(\Omega) \rangle + C_4 D_5 \langle \hat{H}_i(\Omega) \hat{f}_i(\Omega) \rangle]. \end{aligned} \quad (2.77)$$

Equations (2.76) and (2.77) will be analyzed in Secs. III B and III C. The expressions for the C and D coefficients are given in the Appendix.

III. RESULTS

A. Steady state

When the steady-state equations (2.19), (2.22), (2.24), and (2.47) are solved by the use of (2.3), (2.15)–(2.17), (2.25), and (2.26), the external amplitude r_0 and the internal amplitude, phase factor, and gain, A_0 , ϕ_0 , and G , respectively, can be obtained as functions of the normalized pumping rate R and of the strength and the detuning of the injection signal F_0 and $\Delta\omega$, respectively. Some examples of these functions are shown in Figs. 2–4. The following numerical parameters were assumed for the diode laser: $\tau_{sp}=2 \times 10^{-9}$ s, $\tau_{pe}=2.5 \times 10^{-12}$ s, $\tau_{p0}=10 \times 10^{-12}$ s, $\beta=2 \times 10^{-5}$, $n_{sp}=2$, and $\alpha=2$.

Since the parameters R and F_0 have different dimensions and are of different orders of magnitude, F_0 is normalized according to the following arguments. In the absence of injection, the number of photons inside the cavity is given by

$$n_0(R \neq 0, F_0 = 0) = A_0^2 = R n_{sp} \frac{1 + \beta}{\beta}. \quad (3.1)$$

If a strong resonant injection signal ($\Delta\omega=0$) is applied, so that the number of photons in the cavity that are created through the pumping process is negligible compared with the number of photons that are injected, then the number of photons in the cavity is given by

$$n_0(R = 0, F_0 \neq 0) = \frac{4F_0^2 \tau_p^2}{\tau_{pe}} \frac{1}{1 + \alpha^2}. \quad (3.2)$$

The comparison of Eqs. (3.1) and (3.2) suggests the following normalization of the injection signal (disregarding α):

$$S \equiv \frac{4F_0^2 \beta \tau_p^2}{n_{sp}(1 + \beta)\tau_{pe}} \quad (3.3)$$

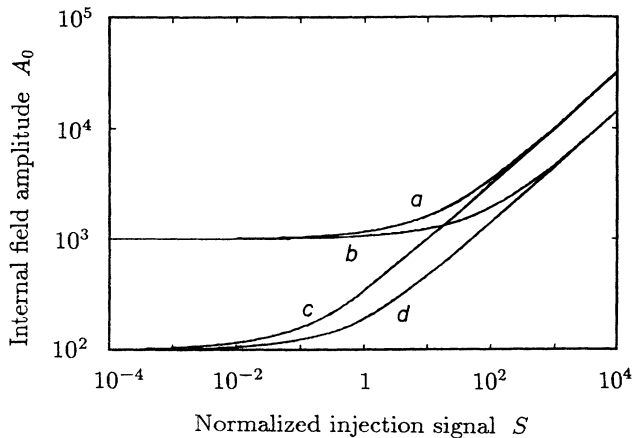


FIG. 2. The internal amplitude as a function of the normalized injection signal with the normalized pumping rate and the linewidth enhancement factor as parameters. $\Delta\omega=0$. *a*, $R=10$, $\alpha=0$; *b*, $R=10$, $\alpha=2$; *c*, $R=0.1$, $\alpha=0$; *d*, $R=0.1$, $\alpha=2$.

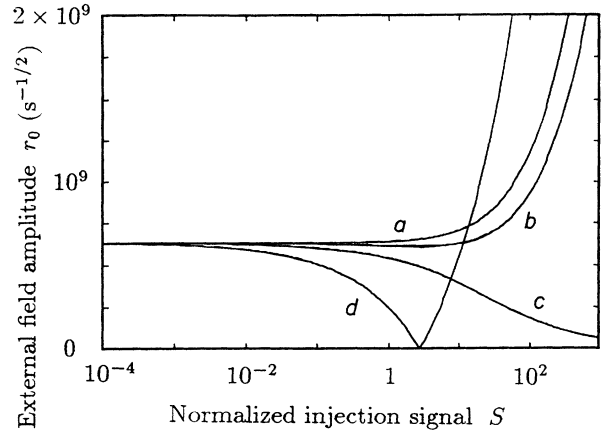


FIG. 3. The external amplitude as a function of the normalized injection signal with the internal losses as a parameter. $R=10$, $\Delta\omega=0$, $\alpha=0$. *a*, $\tau_{pe}/\tau_{p0}=0$; *b*, $\tau_{pe}/\tau_{p0}=\frac{1}{4}$; *c*, $\tau_{pe}/\tau_{p0}=1$; *d*, $\tau_{pe}/\tau_{p0}=4$.

where S is dimensionless.

Figure (2) shows the internal field amplitude A_0 as a function of the injection signal strength for different normalized pumping rates R and linewidth enhancement factors α . The breakpoint where the injection signal starts to dominate over the pump is clearly seen. As expected, it is approximately given by $S=R$ when $\alpha=0$ (curves *a* and *c*), and $\Delta\omega=0$. Around that point, the internal gain G decreases from its initial value of $1/\tau_p$ to zero, cf. Eq. (2.19).

Figure 3 shows the external amplitude r_0 as a function of the normalized injection signal S for varying photon lifetimes due to internal losses τ_{p0} while the photon lifetime due to mirror losses τ_{pe} is constant. If $\tau_{p0} \rightarrow \infty$, i.e., the laser has no internal losses (curve *a*), injection locking will always increase the external amplitude. If the laser

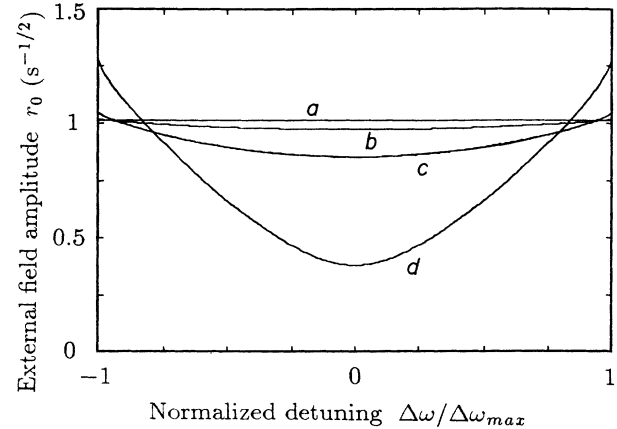


FIG. 4. The normalized external amplitude as a function of the normalized detuning with the internal losses as a parameter. $R=10$, $S=1$, $\alpha=0$. *a*, $\tau_{pe}/\tau_{p0}=0$; *b*, $\tau_{pe}/\tau_{p0}=\frac{1}{4}$; *c*, $\tau_{pe}/\tau_{p0}=1$; *d*, $\tau_{pe}/\tau_{p0}=4$.

on the other hand suffers from internal losses that are smaller than the mirror losses $\tau_{pe} < \tau_{p0} < \infty$ (curve *b*), the external amplitude will increase at strong injection signals after a weak decrease at medium injection signals. When $\tau_{p0} = \tau_{pe}$ (curve *c*), the external amplitude will decrease to zero for high injection signal levels. (In this case, the reflected part of the injection signal interferes destructively with the outgoing part of the laser field, and all injection signal photons are absorbed in the cavity.) Finally, when the internal losses are greater than the mirror losses (curve *d*), the external field amplitude changes sign for some value of the injection. This is a consequence of the fact, that for low injection $S \ll R$ the output consists almost only of photons generated inside the laser, but for high injection $S \gg R$ the output is mainly the reflected injection signal. These two contributions interfere destructively with each other, cf. Eq. (2.44).

The influence of the detuning parameter $\Delta\omega$ on the external amplitude is shown in Fig. 4 for different values of τ_{p0} , while τ_{pe} is constant, in the case of $\alpha=0$. Note that r_0 is normalized by its value at zero injection and that $\Delta\omega$ is normalized by its maximum (positive) value $\Delta\omega_{\max} = F_0 / (A_0 \sqrt{\tau_{pe}})$, cf. Eq. (2.23). The significance of the internal losses is seen: A high τ_{p0} (low internal losses, curve *a*) results in a lower sensitivity to detuning. The reason why r_0 has a minimum when $\Delta\omega=0$ and a maximum when $\Delta\omega=\Delta\omega_{\max}$ is as follows. When $\Delta\omega=0$, the part of the injection signal that enters the cavity is in resonance with the cavity. This part of the injection signal then interferes destructively outside the cavity with the part that is reflected at the input/output mirror. When $\Delta\omega=\Delta\omega_{\max}$ the injection signal is not affected by the gain medium in the cavity. Thus the output signal consists of the reflected injection signal from the input mirror and the light generated inside the cavity, added as intensities. This is obtained from Eq. (2.47) together with $\phi_0 = -\pi/2$ from Eq. (2.22).

B. Noise spectral densities

The external amplitude and phase-noise spectral densities are calculated from Eqs. (2.76) and (2.77). The results for a laser with the above-mentioned numerical parameters are shown in Figs. 5–7 for different injection rates, detunings, squeezing parameters, and linewidth enhancement factors. The calculated Fourier spectra are single sided, normalized spectral densities per hertz as functions of frequency in hertz, cf. Ref. 4.

The normalized external phase-noise spectral density $r_0^2 P_{\Delta\psi}(\Omega)$, where r_0^2 is the normalization factor, is shown in Fig. 5(a) as a function of frequency $\Omega/(2\pi)$. This figure demonstrates that an increasing injection signal decreases the phase noise by several orders of magnitude in the low-frequency region (curves *a* to *d*). When the injection is further increased towards a specific value of S , the relaxation peak increases towards infinity. That tendency is visible in curve *d*, the relaxation peak of which is two orders of magnitude greater than the relaxation peaks of the other curves. This specific value of the injection agrees approximately with the threshold value of the injection for unconditionally stable operation conditions

given in Refs. 11 and 13. In those references it is shown that, when the injection exceeds a threshold value, the positive side and the major part of the negative side (roughly) of the locking bandwidth, cf. Eq. (2.23), are dynamically instable; i.e., small perturbations of the steady-state values of A_0 , N_{c0} , etc. increase exponentially. The unlimited increase of the relaxation peak does not appear at all, if $\alpha=0$.

Figure 5(b) shows the external amplitude noise spectral density $P_{\Delta r}(\Omega)$ as a function of frequency for two different pumping rates with and without pump-noise suppression. The pump-noise suppression is modeled by $\langle \tilde{\Gamma}_p^\dagger(t) \tilde{\Gamma}_p(u) \rangle \equiv 0$, i.e., that the term $p \equiv 0$ in Eq. (2.56), cf. Ref. 4. As can be seen, the amplitude noise in the low-frequency region is slightly increased by the injection signal, both for curves *b* and *d* with pump-noise suppression and for curves *a* and *c* without pump-noise suppression. (The pump-noise was not mentioned in the discussion of Fig. 5(a), because the phase noise is virtually unaffected by the pump-noise suppression.) Again, the relaxation peak shows a strong increase (curves *c* and *d*) when the threshold value of the injection is approached.

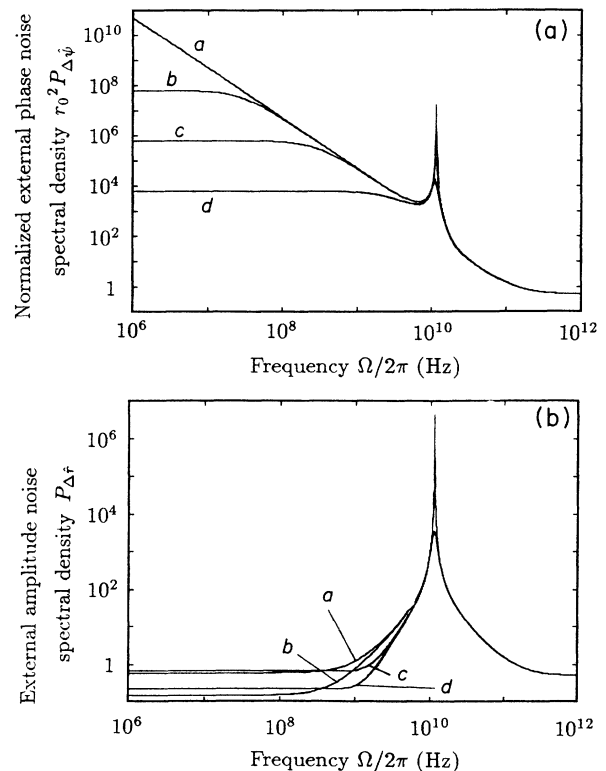


FIG. 5. (a) The normalized external phase-noise spectral density as a function of the frequency with the normalized injection signal as a parameter. $R=10$, $\Delta\omega=0$, $\alpha=2$. *a*, $S=0$; *b*, $S=10^{-6}$; *c*, $S=10^{-4}$; *d*, $S=10^{-2}$. (b) The external amplitude noise spectral density as a function of the frequency with the normalized injection signal as a parameter. $R=1$, $\Delta\omega=0$, $\alpha=2$. *a*, $S=0$, full pump noise; *b*, $S=0$, suppressed pump noise; *c*, $S=10^{-2}$, full pump noise; *d*, $S=10^{-2}$, suppressed pump noise.

The influence of the detuning parameter $\Delta\omega$ at weak injection $S \ll R$ on the noise of a laser without pump-noise suppression in the low-frequency region for different values of α is shown in Figs. 6(a) and 6(b). These figures are drawn for $\Omega/(2\pi)=1$ MHz, which is well below the cavity cutoff and relaxation peak frequencies. As in Fig. 4, $\Delta\omega$ is normalized by its maximum value $\Delta\omega_{\max}$. When the detuning approaches the edge of the locking band (or at least the negative edge if $\alpha \neq 0$), the phase noise Fig. 6(a) and the amplitude noise, Fig. 6(b), increase by several orders of magnitude. A minimum of the amplitude noise is seen close to the negative edge of the locking bandwidth if $\alpha \neq 0$ (or at $\Delta\omega=0$ if $\alpha=0$). At this point $\phi_0 \approx 0$ and $\Delta\omega \approx -\alpha\Delta\omega_{\max}$, cf. Eq. (2.22). This minimum coincides with the dynamically stable operating region given in Refs. 11 and 13. When the injection is increased beyond the above-mentioned threshold value of

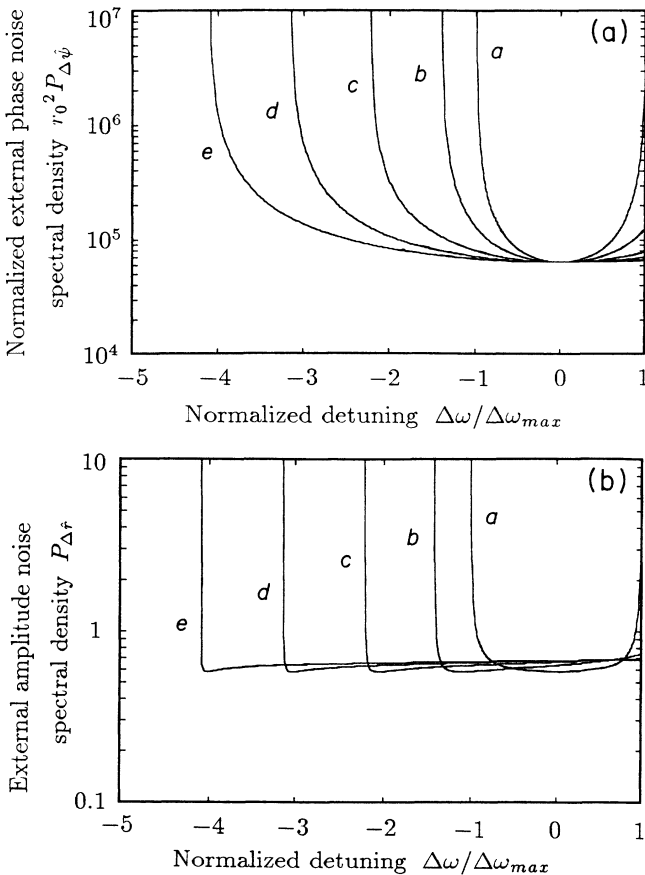


FIG. 6. (a) The normalized external phase-noise spectral density in the low-frequency region [$\Omega/(2\pi)=1$ MHz] as a function of the normalized detuning with the linewidth enhancement factor as a parameter. $R=10$, $S=10^{-3}$. *a*, $\alpha=0$; *b*, $\alpha=1$; *c*, $\alpha=2$; *d*, $\alpha=3$; *e*, $\alpha=4$. (b) The external amplitude noise spectral density in the low-frequency region [$\Omega/(2\pi)=1$ MHz] as a function of the detuning with the linewidth enhancement factor as a parameter. The parameter values are the same as in (a).

the injection, the dynamically stable region in terms of the detuning range $\Delta\omega$ becomes located near the minimum of the amplitude noise, i.e., close to the negative side of the detuning range.

The effect of squeezing the noise of the injection signal of a laser without pump-noise suppression is illustrated in Figs. 7(a) and 7(b) for the low-frequency region [$\Omega/(2\pi)=1$ MHz] with different values of α . Figure 7(a) shows that the normalized phase noise exhibits a minimum at $\kappa \approx \alpha$. (Without injection, i.e., when the input consists of squeezed vacuum, this minimum appears at $\kappa=\alpha$, but when an injection signal is applied, the position of the minimum is a function of both S and $\Delta\omega$. However, in the case of weak injection $S \ll R$ the above-mentioned relation is a good approximation.) The increase in the phase noise for $\kappa \gg 1$ is caused by the increased phase noise of the injection signal. If $\alpha \neq 0$, the phase noise will increase also for $\kappa \ll 1$ because of the coupling of the increased injection signal amplitude noise to fluctuations in the electron population and then to the refractive index and the phase noise of the laser output via the α parameter of the semiconductor laser. Consequently, if the phase noise of the laser output is supposed to be minimized for a laser with $\alpha > 1$, it is better to

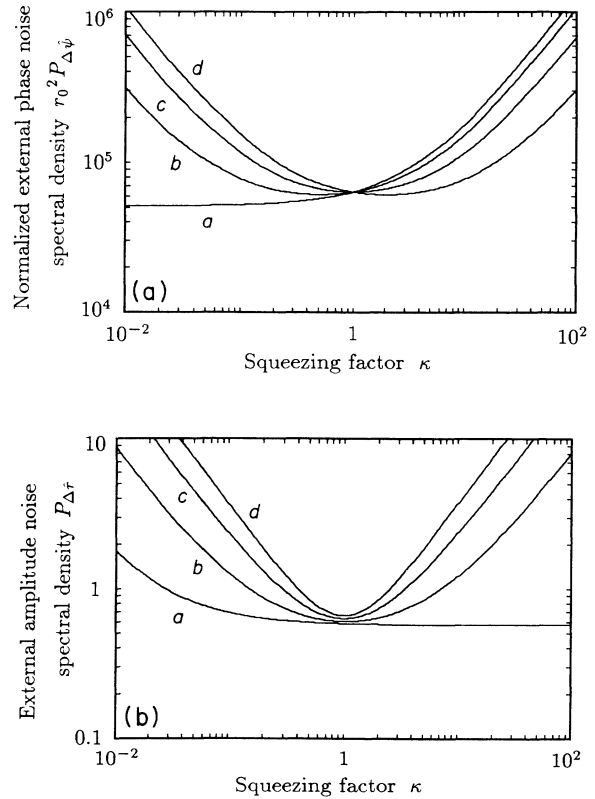


FIG. 7. (a) The normalized external phase-noise spectral density in the low-frequency region [$\Omega/(2\pi)=1$ MHz] as a function of the squeezing with the linewidth enhancement factor as a parameter. $R=1$, $S=10^{-3}$, $\Delta\omega=0$. *a*, $\alpha=0$; *b*, $\alpha=0.5$; *c*, $\alpha=1$; *d*, $\alpha=2$. (b) The external amplitude noise spectral density in the low-frequency region [$\Omega/(2\pi)=1$ MHz] as a function of the squeezing. The parameter values are the same as in (a).

reduce the amplitude noise of the injection signal instead of reducing its phase noise. Figure 7(b) shows the corresponding amplitude noise, which increases when the noise of the injection signal amplitude increases above the noise of a coherent state $\kappa < 1$, regardless of the value of α . When $\alpha = 0$ (curve *a*), the amplitude noise is almost constant for $\kappa > 1$. On the other hand when $\alpha \neq 0$ (curves *b* to *d*), the amplitude noise increases also for $\kappa > 1$. This increase is suppressed if, instead of $\Delta\omega = 0$, a value of $\Delta\omega$ in the vicinity of the amplitude noise minimum in Fig. 6(b) is chosen. In that case, the curves *b* to *d* will coincide with curve *a* in Fig. 7(b). As discussed above, detuning to the amplitude noise minimum implies that $\phi_0 \approx 0$, whereas injection at $\Delta\omega = 0$ implies that $\phi_0 = -\arctan\alpha$ from Eq. (2.22). That is a way of regarding detuning to the amplitude noise minimum as a more natural point of injection than at $\Delta\omega = 0$. In addition, the point $\Delta\omega = 0$ might be dynamically unstable, as mentioned before.

C. Spectral uncertainty product

The normalized external spectral uncertainty product, which is denoted by Π , is defined as

$$\Pi(\Omega) \equiv 4P_{\Delta\hat{r}}(\Omega)r_0^2P_{\Delta\hat{\psi}}(\Omega). \quad (3.4)$$

According to the Heisenberg uncertainty relation, it has a minimum value of 1 for any frequency (cf. Ref. 4). We intend to calculate the normalized uncertainty product in the low-frequency region ($\Omega \ll 1/\tau_{pe}$), in order to find its lowest value for an injection-locked laser oscillator. In Ref. 4 this was shown to be equal to 2 in the frequency region below the relaxation peak for an ideal free-running laser. The low-frequency limit of this region will expand towards dc, when the pumping rate approaches infinity. Thus, a laser without injection locking can never achieve an uncertainty product, that is less than twice the minimum-uncertainty product imposed by the Heisenberg uncertainty relation.

To simplify the calculation of Π , first we assume that we are dealing with a laser with idealized characteristics like in Ref. 4, i.e., $n_{sp} = 1$, $\alpha = 0$, and $\tau_{p0} \rightarrow \infty$. The first condition means that the laser exhibits an ideal population inversion, i.e., the stimulated absorption rate is equal to zero. The second condition implies that the variations of gain and refractive index in the laser are decoupled. The last condition states that the internal losses are negligible as compared to the mirror losses, i.e., that all photons inside the cavity will decay through mirror coupling losses. Furthermore, we assume that the laser is pump-noise suppressed. In addition, high pumping ($R \rightarrow \infty$) and high signal injection ($S \rightarrow \infty$) with perfect matching with the cavity resonance frequency ($\Delta\omega = 0$) is assumed. Under these idealized circumstances, the external amplitude and normalized phase-noise spectral densities are obtained as

$$P_{\Delta\hat{r}}(\Omega \rightarrow 0) = \frac{1}{2\kappa} \left[\frac{\xi}{1-\xi} \right]^2, \quad (3.5)$$

$$r_0^2P_{\Delta\hat{\psi}}(\Omega \rightarrow 0) = \frac{\kappa(1-\xi)^2 + 1 - 2\xi}{2\xi^2}, \quad (3.6)$$

in the low-frequency region. Here we have introduced the parameter ξ , which depends on the internal amplitude and the injection according to

$$\xi = \frac{F_0\sqrt{\tau_{pe}}}{A_0} = \frac{1}{1 + \left[1 + \frac{4R}{S} \right]^{1/2}}. \quad (3.7)$$

From the definition (3.7) we can deduce that $\xi(S/R \rightarrow 0) = 0$ and $\xi(S/R \rightarrow \infty) = \frac{1}{2}$. The normalized external uncertainty product then becomes

$$\Pi(\Omega \rightarrow 0) = 1 + \frac{1 - 2\xi}{\kappa(1-\xi)^2} \geq 1. \quad (3.8)$$

The last inequality means that the laser never violates the Heisenberg uncertainty relation. From this equation it is seen that squeezing of the amplitude noise of the incoming light would lower the uncertainty product as would increasing injection signal. [The function $\Pi(\xi)$, given by Eq. (3.8), decreases monotonically as ξ increases.]

The spectra of $\Pi(\Omega)$, $r_0^2P_{\Delta\hat{\psi}}(\Omega)$, and $P_{\Delta\hat{r}}(\Omega)$ for these idealized conditions are shown in Figs. 8(a), 8(b), and 8(c), respectively. Figure 8(a) shows the normalized uncertainty product as a function of frequency for different injection levels. Without injection, curve *a*, the uncertainty product is equal to 2 in the medium-frequency region, as expected. When the injection is increased, at first the product decreases in the low-frequency part until it acquires the same value as in the medium-frequency part of the spectrum (curves *c* and *d*). That point is equal to the breakpoint $S \approx R$ discussed in Sec. III A. If the injection is further increased, the uncertainty approaches unity in the low- and medium-frequency parts, as the injection approaches infinity (curves *e* and *f*). Consequently, as predicted by Eq. (3.8), the laser never violates the Heisenberg uncertainty relation. As can be deduced from Fig. 8(a), Eq. (3.8) is valid in the low-frequency region only when the value of S exceeds R .

The phase noise of an ideal laser (with or without pump-noise suppression), shown in Fig. 8(b), is decreased for low frequencies by increasing injection, as in the case of a nonideal laser, cf. Fig. 5(a). When $S \rightarrow \infty$, the normalized phase noise approaches $\frac{1}{2}$ (the standard quantum limit) for all frequencies, curve *f*. This is due to the fact that for high injections, the laser output amplitude and noise are completely determined by the injection amplitude and noise, since the contributions generated by pumping are negligible.

The corresponding amplitude noise spectra are shown in Fig. 8(c). It shows that increasing injection increases the amplitude noise in the low-frequency region, that has been reduced by the pump-noise suppression (curves *a* to *f*), cf. Ref. 4. As in the case of the phase noise, for extremely high injection the amplitude noise equals $\frac{1}{2}$ over the entire spectrum, curve *f*. This can be explained in the following way. In Eq. (2.76), the only surviving terms for the ideal injection locked laser in the low-frequency limit are parts of the noise terms $P_{\hat{F}_c}$, $P_{\hat{H}_r}$, $P_{\hat{F}_r}$, and $\langle \hat{H}_r \hat{F}_r \rangle$. At zero injection, the terms $P_{\hat{H}_r}$, $P_{\hat{F}_r}$, and

$\langle \hat{H}_r, \hat{f}_r \rangle$ cancel each other exactly, and the only surviving noise source is the spontaneous emission noise in $P_{\bar{F}_c}$. This is the term proportional to N_{c0}/τ_{sp} in Eq. (2.60), which becomes equal to $1/(2R)$, cf. curve *a*. Accordingly, the vacuum fluctuations that enter the cavity and give rise to amplitude noise interfere destructively with the

part of the vacuum fluctuations that are reflected at the input mirror, giving a result of exactly zero. On the other hand, when the injection approaches infinity, the contribution from $P_{\bar{F}_c}$ is negligible, but the other three terms do not cancel each other. The perfect destructive interference between the noise contributions from the vacu-

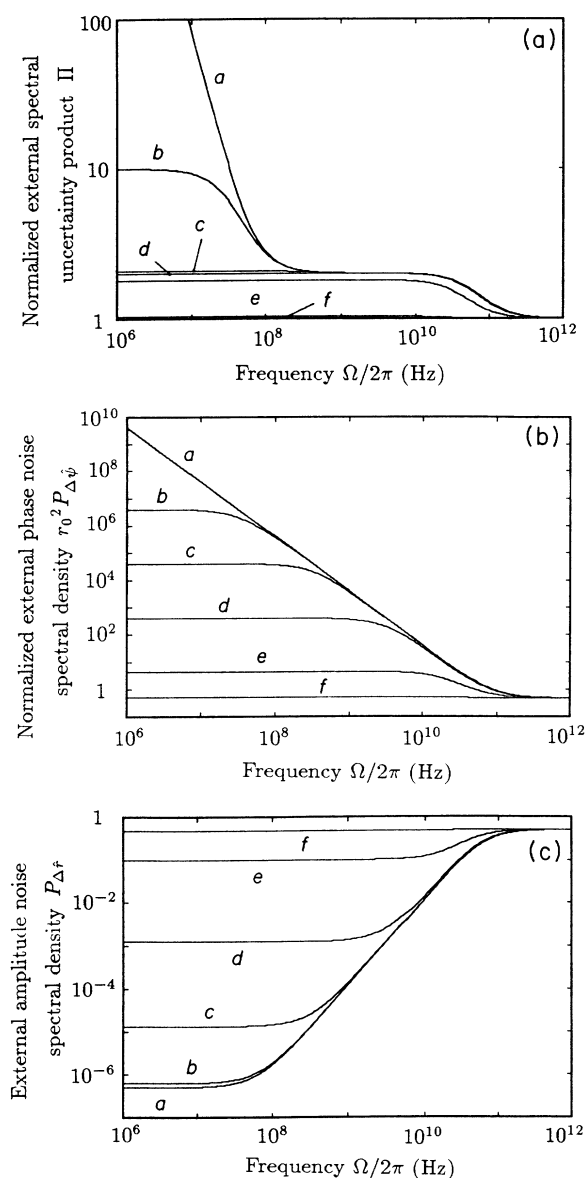


FIG. 8. (a) The normalized external uncertainty product for an ideal laser [$n_{sp}=1$, $\alpha=0$, $\tau_{p0} \rightarrow \infty$, $\langle \bar{\Gamma}_p^\dagger(t) \bar{\Gamma}_p(u) \rangle \equiv 0$] as a function of the frequency with the normalized injection signal as a parameter. $R=10^6$, $\Delta\omega=0$, $\kappa=1$. *a*, $S=0$; *b*, $S=1$; *c*, $S=10^2$; *d*, $S=10^4$; *e*, $S=10^6$; *f*, $S=10^8$. (b) The normalized external phase-noise spectral density for an ideal laser as a function of the frequency with the normalized injection signal as a parameter. The parameter values are the same as in (a). (c) The external amplitude noise spectral density for an ideal laser as a function of the frequency with the normalized injection signal as a parameter. The parameter values are the same as in (a).

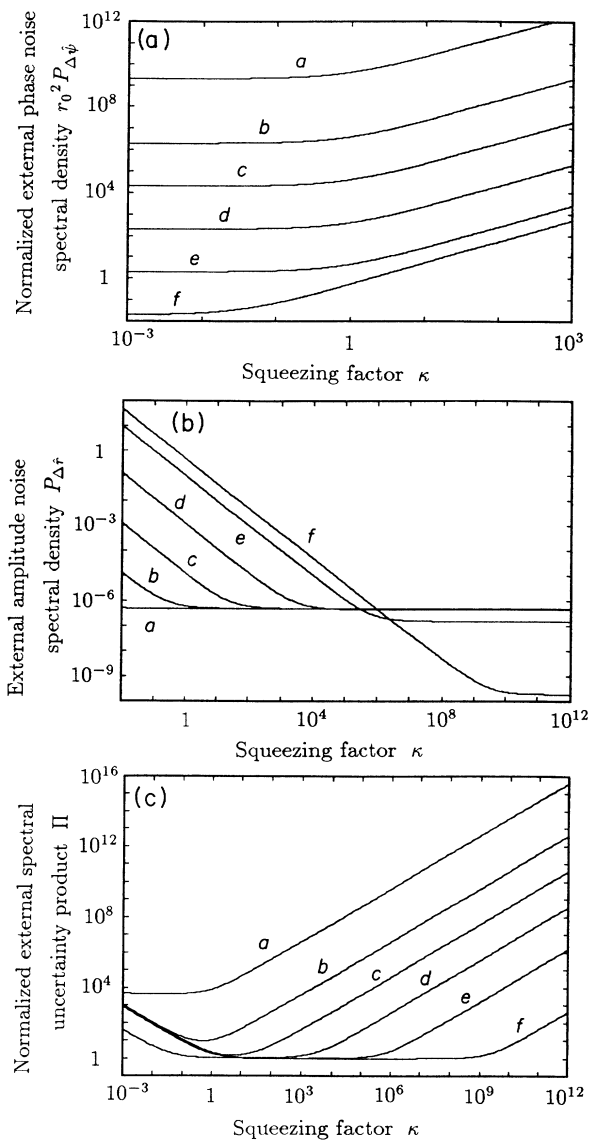


FIG. 9. (a) The normalized external phase-noise spectral density for an ideal laser in the low-frequency region [$\Omega/(2\pi)=1$ MHz] as a function of the squeezing with the normalized injection signal as a parameter. $R=10^6$, $\Delta\omega=0$. *a*, $S=0$; *b*, $S=1$; *c*, $S=10^2$; *d*, $S=10^4$; *e*, $S=10^6$; *f*, $S=10^8$. (b) The external amplitude noise spectral density for an ideal laser in the low-frequency region [$\Omega/(2\pi)=1$ MHz] as a function of the squeezing with the normalized injection signal as a parameter. The parameter values are the same as in (a). (c) The normalized external uncertainty product for an ideal laser in the low-frequency region [$\Omega/(2\pi)=1$ MHz] as a function of the squeezing with the normalized injection signal as a parameter. The parameter values are the same as in (a).

um fluctuations is thus destroyed. The noise term proportional to $P_{\mathcal{F}_i}$ is left over and becomes equal to $1/(2\kappa)$, cf. curve f . (When the same calculation was performed for an ideal laser *without* pump-noise suppression, all curves coincided with curve f . Consequently, $P_{\Delta\hat{\psi}}(\Omega) \equiv \frac{1}{2}$ for all frequencies and all injections.)

If the decrease of the phase noise and the increase of the amplitude noise with increased injection are compared, the phase-noise reduction dominates, which means that the uncertainty product decreases for increasing injections, as was illustrated in Fig. 8(a). When the injection approaches infinity, both the amplitude and phase-noise spectral densities approach $\frac{1}{2}$ for all frequencies, meaning that the normalized uncertainty product will become equal to unity.

The result of squeezing in an idealized injection-locked laser in the low-frequency region [$\Omega/(2\pi)=1$ MHz] is shown in Figs. 9(a)–9(c). Figure 9(a) shows the phase-noise spectral density, which behaves as predicted by Eq. (3.6), viz. that squeezing the injection phase noise is rewarding to a certain κ value. The part that remains when $\kappa \rightarrow 0$ is the noise from the stimulated emission, i.e., the term proportional to $\langle \tilde{E}_{cv} \rangle$ in Eq. (2.59). If curve a is examined in detail, it is clear that for an ideal laser with only injected vacuum ($S=0$), the phase noise (and thereby the linewidth) can be reduced with a factor of 2 if the vacuum is squeezed, as stated in Ref. 7. This is mathematically obtained if the value of κ is changed from 1 to 0.

The amplitude noise in Fig. 9(b) agrees with Eq. (3.5): The noise can be reduced to an arbitrarily low level by increasing the injection and the pumping rate and reducing the injection amplitude noise. The “floor” that is left when $\kappa \rightarrow \infty$ is the same as in the case of a pump-noise suppressed laser with no injection, viz. the noise from the spontaneous emission. The corresponding normalized external uncertainty product is shown in Fig. 9(c). Again it is clear, that neither high injection nor high squeezing will violate the Heisenberg uncertainty relation.

It should be noted however, that the conditions for obtaining an uncertainty product equal to the minimum-uncertainty value given by the Heisenberg uncertainty relation are rather extreme and not realistic for practical applications. However, these calculations have shown that the model used in this work does not contradict the Heisenberg uncertainty relation. The results for infinite injection were expected, since under those circumstances the laser acts as a mirror with a reflectivity equal to unity that does not add any further noise. Thus, the output signal is an exact replica of the injection signal, and the injection state is obtained at the output.

D. Signal-to-noise ratios

If the injection signal of an injection-locked laser oscillator were phase modulated, what would the noise figure \mathcal{F} of the laser be? The noise figure is defined as the quotient of the signal-to-noise ratio (SNR) at the input and the signal-to-noise ratio at the output. This was calculated by using $P_{\mathcal{F}_i}(\Omega)$ as the noise of the input signal and

$P_{\Delta\hat{\psi}}(\Omega)$ as the noise of the output signal. The transfer function for the signal spectral density was computed by using $P_{\mathcal{F}_i}(\Omega)$ as a white input source while all other noise sources were set to zero. Figure 10 shows \mathcal{F} as a function of S with R as a parameter for an ideal laser. It is seen that the laser works as a phase preserving amplifier⁸ that amplifies the signal several orders of magnitude, adding a factor of 2 in noise (3 dB). For high injection, \mathcal{F} becomes equal to unity, but on the other hand the laser does not amplify the signal, but it merely acts as a mirror. Also, if $\kappa \rightarrow \infty$ then $\mathcal{F} \rightarrow 1$ even for low injection. However, this is not a useful alternative, since the carrier frequency then has a completely undetermined phase.

IV. CONCLUSIONS

The amplitude and phase components of the quantum fluctuations of an injection-locked semiconductor laser were calculated using a Langevin operator equation approach based on Ref. 14.

For an ideal diode laser (including pump-noise suppression) the effect of the injection locking using a coherent field was shown to be that the phase noise in the low-frequency region can be suppressed by several orders of magnitude. However, the low amplitude noise originally accomplished by the pump-noise suppression was increased by the injection locking, because the noise was increasingly determined by the injection signal noise alone, which was equal to the standard quantum limit. For extremely strong injection, the output signal was in a minimum uncertainty state for all frequencies with the noise distributed equally between the two quadratures, and the spectral uncertainty product was demonstrated to approach the minimum value allowed by Heisenberg’s uncertainty relation. One should bear in mind, however, that in such cases the output field is always more or less equal to the injection field.

The ideal laser always exhibits the best noise performance at zero detuning, since $\alpha=0$. At the endpoints of the locking frequency range, both the amplitude and the

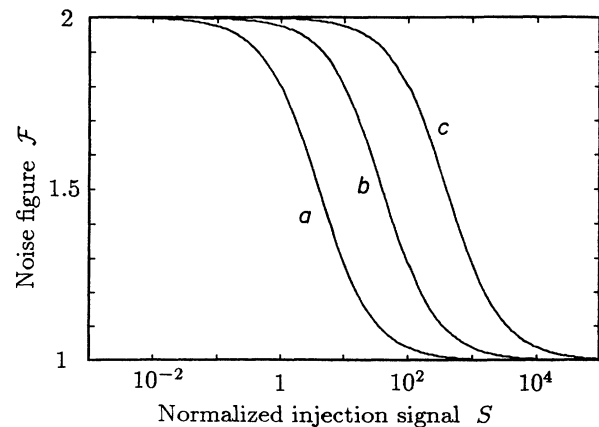


FIG. 10. The noise figure for an ideal laser for amplification of the quadrature-phase component as a function of the normalized injection rate with the normalized pumping rate as a parameter. $\Delta\omega=0$, $\kappa=1$. a , $R=1$; b , $R=10$; c , $R=10^2$.

phase noise in the low frequency region increase by several orders of magnitude. Squeezing of the injection signal for a pump-noise suppressed ideal laser was shown to give a clear redistribution of the noise in the external field, meaning that either the amplitude or the phase noise can be reduced at the expense of the other. If the input is squeezed vacuum, the phase noise (and thus the linewidth) can be reduced by a factor of 2. Using squeezed light input, it is still not possible to violate Heisenberg's uncertainty relation.

A nonideal laser behaves much in the same way as an ideal laser when it comes to detuning as long as its linewidth enhancement factor is equal to zero. If $\alpha > 0$, however, the amplitude noise minimum in the low-frequency region lies close to the lower bandwidth edge (negative detuning), so a precise adjustment of the injection signal frequency is crucial, if the lowest possible amplitude noise is desired. The minimum phase noise is still found at zero detuning.

If the injection signal to a nonideal laser is squeezed, the results differ from squeezing the injection of an ideal laser. The phase noise of the nonideal laser can be slightly reduced in the low-frequency region by squeezing the appropriate quadrature of the injection field. The minimum is reached approximately when $\kappa = \alpha$. This implies that for values of $\alpha > 1$, the minimum signal quadrature-phase noise is obtained when the in-phase amplitude fluctuations of the injection signal are reduced. The simple explanation for this is that the nonzero linewidth enhancement factor couples both the amplitude and the phase noise of the injection signal to the quadrature component of the signal by unequal factors. If the amplitude fluctuations of the output signal are to be minimized, a different procedure has to be employed. If $\alpha \neq 0$, detuning towards the negative edge of the locking bandwidth $\Delta\omega \approx -\alpha\Delta\omega_{\max}$ making $\phi_0 \approx 0$, is required for obtaining the optimum amplitude noise condition. Then, if the amplitude noise of the injection signal is squeezed, it is possible to further decrease the amplitude noise of the laser.

Calculations of the noise figure of the quadrature-phase component was carried out for an ideal laser. As pointed out before, an injection-locked laser will work as a phase preserving amplifier. While being able to amplify the phase information of a signal by several orders of magnitude, the device adds 3 dB excess noise. The excess noise approaches zero when the total gain of the device approaches unity, i.e., for high injection.

ACKNOWLEDGMENTS

The authors would like to thank Professor Olle Nilsson at the Department of Microwave Engineering and Fibre Optics at the Royal Institute of Technology for valuable discussions.

APPENDIX

Here we give the expressions for the B , C , and D coefficients used in Sec. II.

$$B_1 = A_2 A_3 A_5 + A_1 (A_5^2 + A_6^2) - A_0 A_2 A_4 A_6 + \Omega^2 (2A_5 - A_1), \quad (\text{A1})$$

$$B_2 = \Omega (A_2 A_3 + 2A_1 A_5 - A_5^2 - A_6^2 + \Omega^2), \quad (\text{A2})$$

$$B_3 = A_0 A_4 A_6 - A_3 A_5, \quad (\text{A3})$$

$$B_4 = -\Omega A_3, \quad (\text{A4})$$

$$B_5 = A_1 A_6, \quad (\text{A5})$$

$$B_6 = -\Omega A_6, \quad (\text{A6})$$

$$B_7 = A_1 A_5 + \Omega^2, \quad (\text{A7})$$

$$B_8 = \Omega (A_1 - A_5), \quad (\text{A8})$$

$$B_9 = A_0 B_2 \Omega (A_1 - A_5) - A_0 B_1 (A_1 A_5 + \Omega^2), \quad (\text{A9})$$

$$B_{10} = A_0 B_1 \Omega (A_5 - A_1) - A_0 B_2 (A_1 A_5 + \Omega^2), \quad (\text{A10})$$

$$B_{11} = B_3 (A_0 A_2 A_4 - A_1 A_6) - A_6 B_4 \Omega + A_0 A_4 B_1, \quad (\text{A11})$$

$$B_{12} = B_4 (A_0 A_2 A_4 - A_1 A_6) + A_6 B_3 \Omega + A_0 A_4 B_2, \quad (\text{A12})$$

$$B_{13} = B_7 (A_0 A_2 A_4 - A_1 A_6) - A_6 B_8 \Omega, \quad (\text{A13})$$

$$B_{14} = B_8 (A_0 A_2 A_4 - A_1 A_6) + A_6 B_7 \Omega, \quad (\text{A14})$$

$$B_{15} = B_5 (A_0 A_2 A_4 - A_1 A_6) - A_6 B_6 \Omega + A_1 B_1 + \Omega B_2, \quad (\text{A15})$$

$$B_{16} = B_6 (A_0 A_2 A_4 - A_1 A_6) + A_6 B_5 \Omega + A_1 B_2 - \Omega B_1, \quad (\text{A16})$$

$$C_5 = \frac{1}{C_3^2 + C_4^2} \equiv \frac{1}{r_0^2}, \quad (\text{A17})$$

$$C_6 = -C_2 F_0, \quad (\text{A18})$$

$$C_7 = C_3^2 + C_4 (C_4 + F_0), \quad (\text{A19})$$

$$C_8 = \frac{r_0}{C_4}, \quad (\text{A20})$$

$$C_9 = C_1 + C_3 C_5 C_6, \quad (\text{A21})$$

$$C_{10} = C_3 (C_5 C_7 - 1), \quad (\text{A22})$$

$$C_{11} = C_3^2 C_5 - 1, \quad (\text{A23})$$

$$C_{12} = C_3 C_4 C_5, \quad (\text{A24})$$

$$C_{13} = C_5 C_6, \quad (\text{A25})$$

$$C_{14} = C_5 C_7, \quad (\text{A26})$$

$$C_{15} = B_1^2 + B_2^2, \quad (\text{A27})$$

$$C_{16} = B_9^2 + B_{10}^2, \quad (\text{A28})$$

$$C_{17} = C_8 C_9, \quad (\text{A29})$$

$$C_{18} = C_8 C_{10}, \quad (\text{A30})$$

$$D_1 = \frac{C_{13}}{C_{15}}(B_1 B_3 + B_2 B_4) + \frac{C_{14}}{C_{16}}(B_9 B_{11} + B_{10} B_{12}), \quad (\text{A31})$$

$$D_7 = \frac{C_{17}}{C_{15}}(B_1 B_3 + B_2 B_4) + \frac{C_{18}}{C_{16}}(B_9 B_{11} + B_{10} B_{12}), \quad (\text{A37})$$

$$D_2 = \frac{C_{13}}{C_{15}}(B_1 B_4 - B_2 B_3) + \frac{C_{14}}{C_{16}}(B_9 B_{12} - B_{10} B_{11}), \quad (\text{A32})$$

$$D_8 = \frac{C_{17}}{C_{15}}(B_1 B_4 - B_2 B_3) + \frac{C_{18}}{C_{16}}(B_9 B_{12} - B_{10} B_{11}), \quad (\text{A38})$$

$$D_3 = \frac{C_{13}}{C_{15}}(B_1 B_7 + B_2 B_8) + \frac{C_{14}}{C_{16}}(B_9 B_{13} + B_{10} B_{14}), \quad (\text{A33})$$

$$D_9 = \frac{C_{17}}{C_{15}}(B_1 B_7 + B_2 B_8) + \frac{C_{18}}{C_{16}}(B_9 B_{13} - B_{10} B_{14}), \quad (\text{A39})$$

$$D_4 = \frac{C_{13}}{C_{15}}(B_1 B_8 - B_2 B_7) + \frac{C_{14}}{C_{16}}(B_9 B_{14} - B_{10} B_{13}), \quad (\text{A34})$$

$$D_{10} = \frac{C_{17}}{C_{15}}(B_1 B_8 - B_2 B_7) + \frac{C_{18}}{C_{16}}(B_9 B_{14} - B_{10} B_{13}), \quad (\text{A40})$$

$$D_5 = \frac{C_{13}}{C_{15}}(B_1 B_5 + B_2 B_6) + \frac{C_{14}}{C_{16}}(B_9 B_{15} + B_{10} B_{16}), \quad (\text{A35})$$

$$D_{11} = \frac{C_{17}}{C_{15}}(B_1 B_5 + B_2 B_6) + \frac{C_{18}}{C_{16}}(B_9 B_{15} + B_{10} B_{16}), \quad (\text{A41})$$

$$D_6 = \frac{C_{13}}{C_{15}}(B_1 B_6 - B_2 B_5) + \frac{C_{14}}{C_{16}}(B_9 B_{16} - B_{10} B_{15}), \quad (\text{A36})$$

$$D_{12} = \frac{C_{17}}{C_{15}}(B_1 B_6 - B_2 B_5) + \frac{C_{18}}{C_{16}}(B_9 B_{16} - B_{10} B_{15}). \quad (\text{A42})$$

¹H. Yuen, *Phys. Rev. A* **13**, 2226 (1976).

²D. Walls, *Nature (London)* **306**, 5141 (1983).

³J. Opt. Soc. Am. **B 4** (1987), special issue on squeezed states of the electromagnetic field.

⁴Y. Yamamoto, S. Machida, and O. Nilsson, *Phys. Rev. A* **34**, 4025 (1986).

⁵Y. Yamamoto and S. Machida, *Phys. Rev. A* **35**, 5114 (1987).

⁶M. Marte, H. Ritsch, and D. Walls, *Phys. Rev. Lett.* **61**, 1093 (1988).

⁷J. Gea-Banacloche, *Phys. Rev. Lett.* **59**, 543 (1987).

⁸H. A. Haus and Y. Yamamoto, *Phys. Rev. A* **29**, 1261 (1984).

⁹C. H. Henry, *IEEE J. Quantum Electron.* **QE-18**, 259 (1982).

¹⁰R. Lang, *IEEE J. Quantum Electron.* **QE-18**, 976 (1982).

¹¹F. Mogensén, H. Olesen, and G. Jacobsen, *IEEE J. Quantum Electron.* **QE-21**, 784 (1985).

¹²P. Spano, S. Piazzolla, and M. Tamburrini, *IEEE J. Quantum Electron.* **QE-22**, 427 (1986).

¹³I. Petitbon, P. Gallion, G. Debarge, and C. Chabran, *IEEE J. Quantum Electron.* **24**, 148 (1988).

¹⁴Y. Yamamoto and N. Imoto, *IEEE J. Quantum Electron.* **QE-22**, 2032 (1986).

¹⁵D. T. Pegg and S. M. Barnett, *Phys. Rev. A* **39**, 1665 (1989).